Femtosecond laser studies of the relaxation dynamics of semiconductors and large molecules

by C. L. Tang F. W. Wise M. J. Rosker I. A. Walmsley

The use of femtosecond lasers and the related optical correlation spectroscopic technique for studying the relaxation dynamics of semiconductors and photoexcited molecules are reviewed. In particular, the results on the intraband relaxation of nonequilibrium carriers in GaAs and related compounds and quantum well structures are summarized. The optical correlation technique also led to the observation of quantum beats in the femtosecond time domain corresponding to the direct observation of molecular vibrations in the time domain.

1. Introduction

Femtosecond lasers and related optical techniques have recently been used successfully to study a variety of ultrafast relaxation processes in semiconductors and molecules. In the

©Copyright 1989 by International Business Machines Corporation. Copying in printed form for private use is permitted without payment of royalty provided that (1) each reproduction is done without alteration and (2) the *Journal* reference and IBM copyright notice are included on the first page. The title and abstract, but no other portions, of this paper may be copied or distributed royalty free without further permission by computer-based and other information-service systems. Permission to *republish* any other portion of this paper must be obtained from the Editor.

case of semiconductors, extensive studies have been carried out on the intraband relaxation dynamics of nonequilibrium carriers in GaAs and related compounds and structures, such as $Al_xGa_{1-x}As/GaAs$ quantum wells and superlattices. In the case of molecules, femtosecond quantum beats corresponding to molecular vibrations in large organic molecules have been observed directly in the time domain for the first time.

There are two basic approaches to the study of the relaxation dynamics of nonequilibrium carriers in semiconductors. In the first approach, the emphasis is on the transport properties of the carriers. In structures such as the tunneling hot-electron transfer amplifier (or THETA devices), electrons are injected into a drift region of the order of the mean free path or shorter, and then collected. The relaxation or transport properties of the injected carriers in the drift region are usually inferred from the measured properties of the overall structure, including the injection, drift, and collection regions. This requires a detailed knowledge of the injection and collection processes which can complicate the interpretation of the data. In the second approach, nonequilibrium carriers are created in a volume with dimensions large compared to the mean free path of the carriers. Carrier dynamics are determined through time-



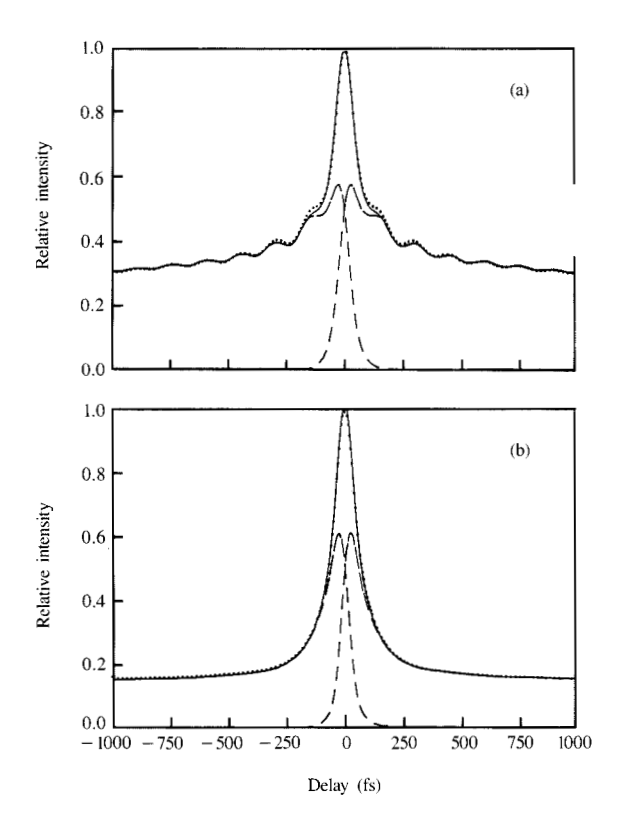


Figure 1

Comparisons of pump-probe and transmission-correlation experimental results. The symbols represent the transmission-correlation peak (TCP) signals, and the dashed lines represent the two pump-probe (PP) signals. That is, for positive delays the transmission of pulse B (see text) is measured, and for negative delays that of pulse A is measured. The solid lines are the sum of the two PP signals which reproduce the corresponding TCPs. The sample in (a) was a $2-\mu m$ jet of solution of Ethyl Violet, and that in (b) was a $0.2-\mu m$ -thick film of $Al_{0.35}Ga_{0.65}As$.

dependent measurements requiring measurement techniques and sources with femtosecond time resolution. Recent developments in femtosecond lasers and related optical measurement techniques have made such time-dependent measurements possible. The spatial and time domain measurements complement each other. At the present time, the accuracy of the time-domain measurement of the relaxation times of nonequilibrium carriers appears to be the better of the two.

Such time-dependent measurements have led to a fairly consistent and complete picture of the relaxation dynamics of the photo-excited carriers out of the initial states in GaAs and related materials and quantum well structures. Many of these results have now been substantiated by other

independent experiments and by extensive Monte Carlo calculations. In this paper, we review these techniques and the results obtained, mainly those at the authors' laboratory at Cornell University, on the relaxation dynamics of nonequilibrium carriers in semiconductors and quantum beats in large molecules.

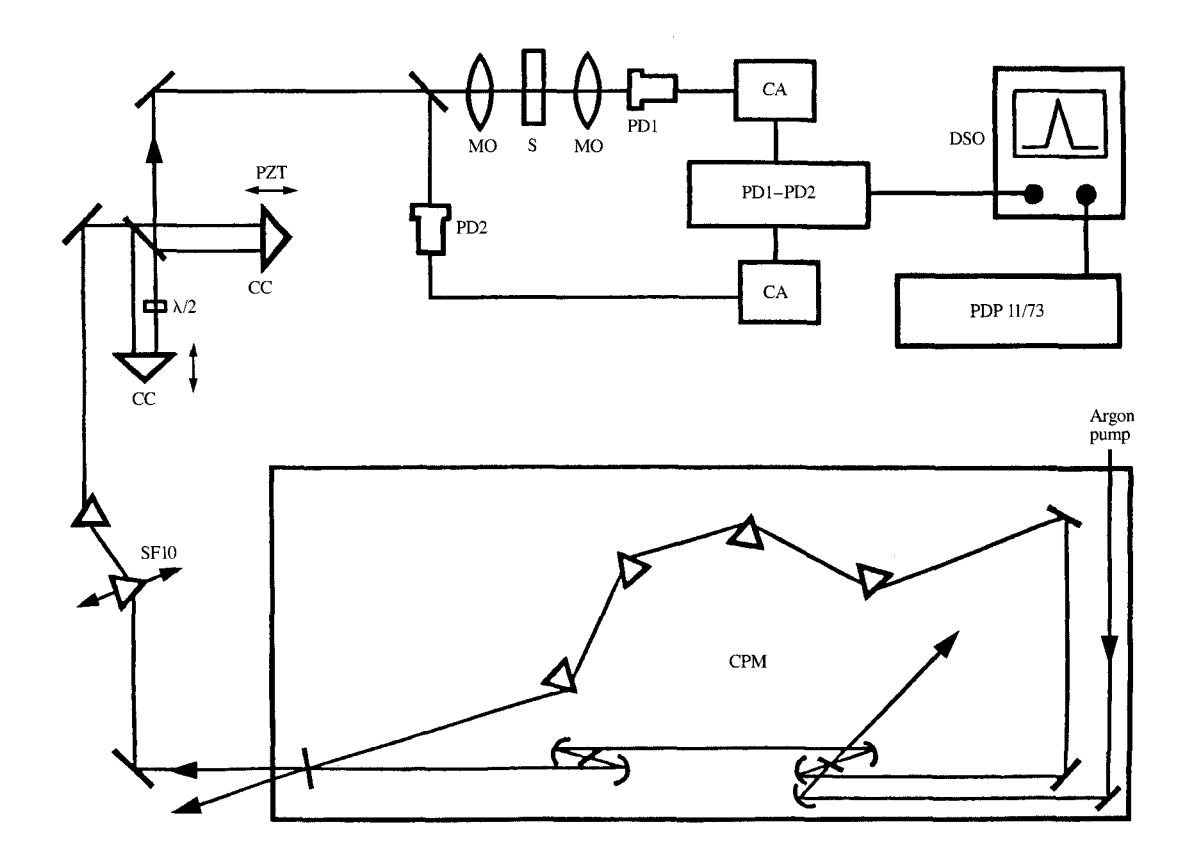
2. Experiment

• Optical correlation spectroscopy

The basic optical technique most commonly used for studying ultrafast relaxation dynamics is the pump-probe technique. This is a generic name for the type of measurements where the material system to be studied is first perturbed or excited by a short "pump" pulse, and the response of the system is then measured by observing the effects of the perturbed system on suitably time-delayed probe pulses. Experimentally, the problem is often complicated because the response of the system may consist of processes with relaxation times ranging from as short as the optical pulse width to those much longer than the scanning time of the experiment. To separate out the fast processes in the presence of the slow processes may require extensive preprocessing of the data. The optical correlation technique automatically removes the effects of the slow processes from the data experimentally and allows the data which contain only the effects of the fast processes to be analyzed directly without the need for any preprocessing.

The optical correlation technique is basically a symmetrized version of the pump-probe technique in the following sense. Again, two short pulses, say pulse A and pulse B, are incident on the sample. The detection system in the case of transmission-correlation experiments measures both the effect of A on B and of B on A. If positive delay is defined as the delay of B from A, then B is the probe pulse for positive delay and A is the probe pulse for negative delay. Thus, in the pump-probe experiments, if A is the pump pulse, only pulse B is detected, whereas in correlation experiments, both pulses A and B are detected for positive and negative delays. To the lowest nonlinear order, the effect of A on B is the same as that of B on A, and the measured correlation trace is symmetric with respect to zero delay between the pulses. Thus, the two-pulse correlation result is simply a symmetrized version of the asymmetric pumpprobe result. Figure 1 shows that this is exactly the case for saturated absorption in large molecules or in semiconductors. Data obtained in these two types of experiments contain, therefore, exactly the same information. The key points of the optical correlation technique are the following:

 The time-origin, or zero delay between the pulses, is automatically determined and obvious from the data, which are symmetric about the zero-delay point.



Schematic of experiment. Key: CPM = colliding pulse-mode-locked ring dye laser; SF10 = SF10 dispersive glass prisms; CC = corner cube; $\lambda/2$ = half-wave plate; MO = microscope objective; S = sample; PD1, PD2 = photodiodes; PZT = piezoelectric transducer; CA = current amplifier, DSO = digital oscilloscope.

- A slow process only gives rise to a constant background shift of the correlation trace. Thus, subtraction of the effects of the slow processes on the time scale of the fast process is automatically accomplished in the experiment.
- 3. The symmetry of the correlation trace is an all-important real-time indicator of whether all the beams are properly aligned. A slight improper alignment of the optical beams can lead to significant errors in the final determination of the time constants when multiple relaxation processes are present. The symmetry of the correlation trace is very sensitive to any misalignment. It serves as an indispensable real-time tool for screening the data sets.

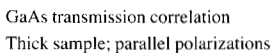
The results reviewed in this paper are based primarily on optical correlation spectroscopy, in particular transmission-correlation spectroscopy.

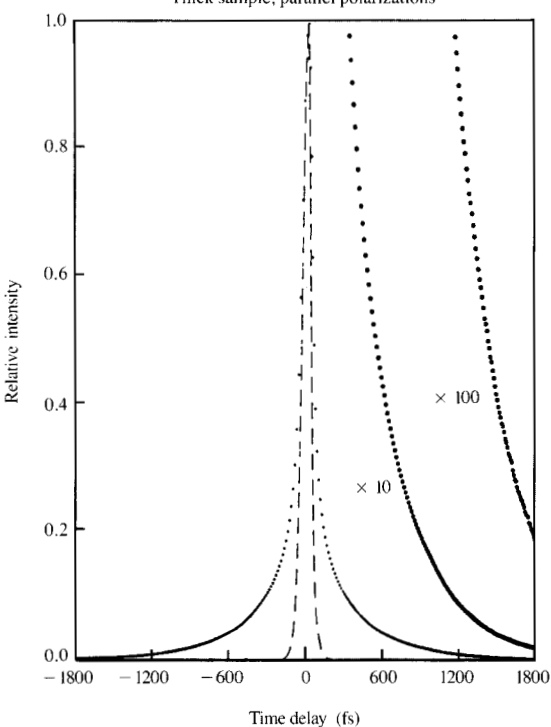
A detailed theory of the transmission-correlation technique is given in [1]. A full density-matrix theory for the transmission-correlation signal, including finite homogeneous and inhomogeneous dephasing and possible quantum beats, is given in [2, 3].

• Experimental setup and procedure

A schematic of the transmission-correlation experiment is shown in Figure 2. Pulses typically 35 femtoseconds long at 10⁸ Hz rate from the dispersion-compensated femtosecond laser (CPM) are split at the interferometer where one of the arms can be scanned by a PZT with a long travel (up to 1 mm). The pulses are then combined and sent through the sample, and the total transmitted power of both pulses is measured as a function of the delay between the two pulses. The result is the transmission-correlation trace, and the peak

449





allellie e

Transmission-correlation trace for thick (\sim 1 μ m) GaAs sample and carrier density of 10^{18} cm $^{-3}$. Only the positive half of the symmetric trace is shown on the expanded scales.

centered on zero delay is the transmission-correlation peak (TCP). More specifically, the transmission-correlation trace is the convolution of the autocorrelation of the incident pulses and the response function of the material. A similar arrangement can be used to measure, for example, the reflection-correlation peak (RCP) instead of the transmission-correlation peak.

Nonlinear saturation in transmission $\Delta T/T$ as small as 10^{-3} with a signal-to-noise ratio of over 60 dB is routinely obtained for GaAs samples 200 to 300 nm thick. Figure 3 shows data with a signal-to-noise ratio of 80 dB. Most groups change the interferometer delay with a stepping motor and use synchronous detection. Because the laser noise is primarily in the low-frequency range, better noise reduction is obtained by simply averaging successive traces through rapid scanning of the interferometer and averaging over a large number of scans per data trace. The piezoelectric transducer in one of the interferometer arms allows rapid scanning up to 6 ps at 10 Hz. The transmission-correlation spectroscopic technique is by now a well-established and

precise experimental technique for acquiring data on ultrafast processes in semiconductors and dye molecules.

◆ Data analysis procedure

To correctly extract multiple relaxation-time constants from the data in the presence of noise is an equally challenging problem [4]. There are several issues involved. The first is that, within the autocorrelation width, the transmissioncorrelation trace generally contains a spurious signal, or the coherent artifact [5, 6]. Second, the excited states usually relax via several channels. The data have to be analyzed without the benefit of prior knowledge of either the number of relaxation channels or the functional form of the time dependence of each individual relaxation process. In fitting the data by multiple exponential decay terms, for example, an incorrect choice in the number of terms can easily lead to significant errors in the amplitudes and the time constants of the exponentials. After extensive numerical evaluations based upon simulated data, we have concluded that the recently developed linear-prediction least-square fitting procedure [4, 7] is a reliable method for analyzing transmission-correlation and also conventional pump-probe types of experiments.

In the linear-prediction procedure, the data are to be fitted to an undetermined number of damped cosinusoidal terms with arbitrary amplitude, damping constant, frequency, and phase:

$$y(t) = \sum_{i=1}^{N} a_i \exp(-t/T_i) \cos(2\pi \nu_i t + \phi_i).$$
 (1)

The linear-prediction procedure yields the number of terms and all four parameters for each term. Note that with the number of terms in the expansion initially unrestricted, the damped cosinusoidal terms form a complete set of functions. It is analogous to the Laplace transform with an arbitrary number of roots. Thus, there is no restriction on the functional form of the relaxation processes. If there is a nonexponential relaxation process, the linear prediction will yield enough complex roots to reproduce the nonexponential function. On the other hand, if the linear-prediction fitting procedure produces a finite and small number of real roots from the data, then the relaxation processes are exponential, consistent with the accuracy of the experimental data. A detailed evaluation of the possible sources of error and the limits of applicability of this procedure is given in [4]. By limiting the data to be used in this procedure to the region outside the autocorrelation width, the coherent artifact problem mentioned earlier is automatically avoided. This truncation of the data places a restriction on the minimum signal-to-noise ratio that can be tolerated and sets a lower limit on the time resolution relative to the pulse width. For typical experiments on GaAs and related compounds and structures and dye molecules, a signal-to-noise ratio of the order of 60 dB is required for an accuracy in the time

Table 1 Summary of decay parameters for photoexcited carriers in semiconductors. Values are given for carrier densities between 7×10^{17} cm⁻³ and 10^{19} cm⁻³. Amplitudes are normalized so that y(t=0) = 1. Parallel and perpendicular polarizations refer to the polarization states of the pump and probe pulses.

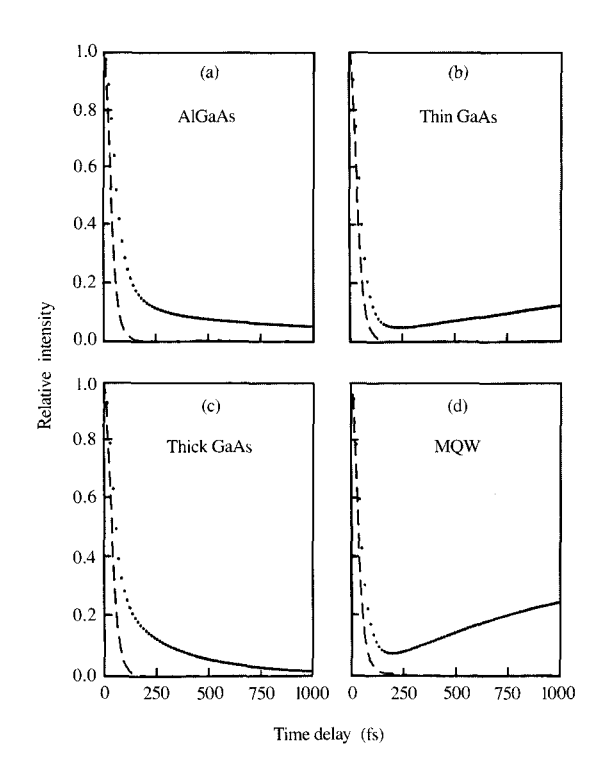
$y(t) = \sum a_i \exp(-t/T_i)$						
Material	Polarization	а	T (fs)			
Al _{0.34} Ga _{0.66} As	Parallel	0.85	40-45			
0.54 0.00		0.10	120-150			
		0.05	1300-1700			
	Orthogonal	0.81	43-48			
	_	0.13	120-150			
		0.06	1500-1800			
GaAs	Parallel	1.02	32-37			
		0.09	140-260			
		-0.11	1600-1900			
	Orthogonal	1.04	37-41			
		0.11	160-260			
		-0.15	1600-1900			
MQW	Parallel	1.67	43-48			
•		-0.67	1500-3000			

constant of the order of 5–10%. The fastest process that can be resolved is of the order of 25 fs for a pulse width of 40 fs at 10^8 Hz rate.

3. Results and discussion

• Intraband relaxation dynamics of nonequilibrium carriers in III-V compounds

With photoexcitation, both nonequilibrium electrons and holes are created in the excited states. However, the hole relaxation rate is expected to be too fast to be seen with the time resolution of our experiment. Also, because of the large difference in the effective masses of the electrons and holes, the nonequilibrium holes are energetically much closer to the top of the valence band than the electrons are to the bottom of the conduction band. The relaxation processes seen are, therefore, primarily those of the electrons. The results on the relaxation dynamics of nonequilibrium electrons initially excited by 2-eV femtosecond pulses in GaAs, Al_{0.34}Ga_{0.66}As, and GaAs/Al_{0.6}Ga_{0.4}As multiple quantum wells (MQW) are summarized in Table 1 [8]. Typical data are shown in Figure 4. The samples are in the form of thin films of the order of 200 to 300 nm thick. The basic results obtained are the same with LPE-, MOCVD-, or MBE-grown samples from various sources. They reflect, therefore, intrinsic properties of the materials studied. For 2-eV photons, the relevant transitions in GaAs and Al_{0.32}Ga_{0.68}As are shown in Figure 5. Note that in the case of GaAs, transitions from the heavy hole, light hole, and split-



Figure

Typical transmission correlation results for (a) $Al_{0.32}Ga_{0.68}As$, (b) $GaAs~(0.3~\mu m~thick)$, (c) $GaAs~(1.1~\mu m~thick)$, (d) $GaAs/Al_{0.6}Ga_{0.4}As~MQW$ structure. Only the positive halves of the symmetric transmission correlation traces are shown. The dashed lines are the pulse autocorrelation, shown for reference.

off bands are energetically possible. In the case of Al_{0.32}Ga_{0.68}As, transition from the split-off band is not allowed.

There are several notable features in the data. In all three cases, there is one dominant fast-relaxation component with a time constant in the range of 35–45 fs. Second, in bulk GaAs and AlGaAs samples there is an intermediate component of the order of 150 to 250 fs. Finally, in the case of AlGaAs at all carrier concentrations but GaAs and MQWs at low photogenerated carrier concentrations (low 10¹⁷ cm⁻³ or below), there is a decay component with a time constant over a picosecond long. In the case of GaAs and MQWs at high concentrations, there is a long component with a time constant of the order of 2 ps and a negative amplitude. This means that the observed transmission-correlation peaks have a rising wing, with a time constant of the order of 2 ps and a peak at 3–5 ps for MQWs and 5–10 ps for GaAs before decaying again to the background level.

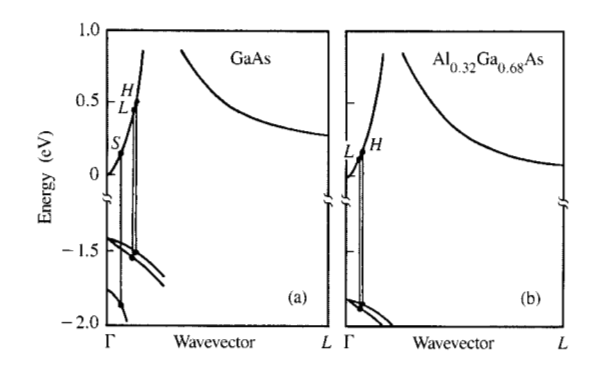


Figure 5

Band structures of (a) GaAs and (b) $AI_{0.32}Ga_{0.68}As$, showing the three valence bands and the central L-valleys of the conduction band. The X-valley is not shown. H, L, and S mark the levels optically coupled by the allowed transitions for a 2.02-eV photon from the heavy-hole, light-hole, and split-off valence bands, respectively, to the conduction band.

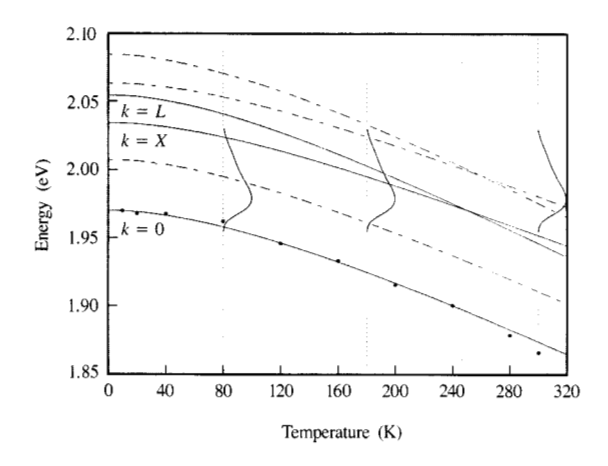


Figure 6

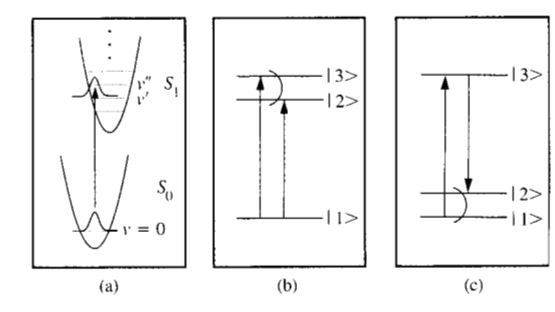
Variation of conduction-band minima (solid lines) with temperature. The symbols are measured values of the energy gap. The dashed lines are one LO-phonon energy above the conduction-band minima. The power spectrum of the laser is plotted at 80, 180, and 300 K. The sample was chemically etched to a thickness of less than one absorption length at 180 K.

The physical mechanisms responsible for these various components are the following. The fast component (35–45 fs) is primarily due to deformation potential scattering from the central Γ -valley to the L- and X-valleys. Because of the

relative densities of states, L-valley scattering dominates. Our results imply a deformation potential constant for L-valley scattering of $D \sim 9 \times 10^8$ eV/cm [8, 9]. A small fraction of the fast component is due to carrier–carrier scattering. The intermediate component (around 200 fs) in GaAs and AlGaAs is due to polar optical phonon scattering within the central valley.

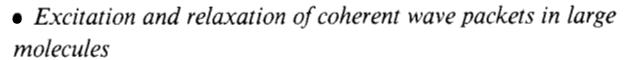
By temperature-tuning the bandgap of Al_{0.35}Ga_{0.65}As from 300 K down to liquid-He temperature (Figure 6) to successively eliminate the possibility of various scattering processes for removing the nonequilibrium electrons from the excited conduction band states by 2-eV photons, we have determined the relative contributions of these processes to the initial decay rate [10]. At a photogenerated carrier concentration of 5×10^{17} cm⁻³, for example, we found that 63% of the electrons have scattered out of the initial states in the first 50 fs. Of these, roughly 65% scatter to the satellite valleys (L and X), 30% leave due to carrier–carrier interaction, and about 5% decay by LO phonon emission. The intermediate component (\sim 200 fs) is not seen in the case of MQWs, because the energy bandwidth of the initially excited states is far greater than the phonon energy of 36 meV. This is because the valence band structure of the MQWs is very complicated [11]. The resulting bandwidth of the optically coupled region in the conduction band is of the order of 200 meV or more. Thus, LO phonon emission does not remove enough of the carriers from the optically coupled region to give rise to a discernible intermediate relaxation component.

The rising-wing component observed in GaAs and GaAs/AlGaAs MQEs at high concentrations is due to saturation of the split-off transition [12], or the dynamic band-filling effect, as the carriers reach the bottom of the Γ valley in GaAs. The carriers scatter from the initially excited states at 0.5 eV mainly to the satellite valleys first. This is quickly followed by relaxation to the bottom of the L-valley and return to the central Γ -valley. However, because of the very large difference between the densities of states in the Land Γ -valleys, the rate of return is limited to the order of (1.65)⁻¹ ps, and it takes 5-10 ps to drain all the carriers in the satellite valleys down the Γ -valley to the bottom. If the carrier concentration is high enough to saturate the split-off transition just above the bottom of the conduction band of GaAs, it leads to a rising-wing component with a time constant of ~ 2 ps and a peak 5-10 ps later. This interpretation is substantiated by the fact that the rising wing is never seen in Al_{0.32}Ga_{0.68}As, where the split-off transition is energetically not allowed. Independent measurements using other techniques have also confirmed this interpretation. In the case of Al_{0.34}Ga_{0.66}As and GaAs or GaAs/AlGaAs MQWs at low photogenerated carrier concentrations, there is also a very weak long decay component with a positive amplitude. The precise physical origin of this component is still not known.



Figure

(a) Schematic showing the excitation of a coherent wave packet in a molecule. The molecule is initially in the ground vibrational state of the ground electronic state. A short pulse excites the molecule into a coherent-superposition vibrational state (or coherent vibrational wave packet of the excited electronic level). This wave packet will oscillate at the vibrational frequency of the molecule, leading to quantum beats in pump-probe or optical-correlation experiments. (b) Three-level model for the excitation of a coherent wave packet in the excited states and the observation of quantum beats. (c) Three-level model for quantum beats due to coherent wave packet oscillation in the ground states created through the resonant Raman process.



A most interesting result in the study of the relaxation dynamics of large molecules following femtosecond photoexcitation is the observation of molecular vibrations directly in the time domain in the form of quantum beats [13, 14].

The relaxation dynamics of photoexcited dye molecules and semiconductors are analogous, where the ground and excited vibronic bands in molecules are analogous, respectively, to the valence and conduction bands in semiconductors. Experimentally, instead of thin films of semiconductors, thin jets of dye molecules dissolved in ethylene glycol with optical densities typically of the order of 0.1 or 0.2 are used. Because the collision time between the solute and solvent molecules is typically of the order of a picosecond or more, the molecules may be considered isolated on a femtosecond time scale, and the relaxation processes immediately following femtosecond pulse excitation are primarily intramolecular processes.

Qualitatively, the short pulse excites the molecules into an excited electronic state and can leave them in a state which is a coherent superposition of adjacent vibrational levels of a particular normal mode of the molecules if the bandwidth of the pulse spans at least two of the vibrational levels. This is illustrated schematically in **Figure 7(a)** in the case of a

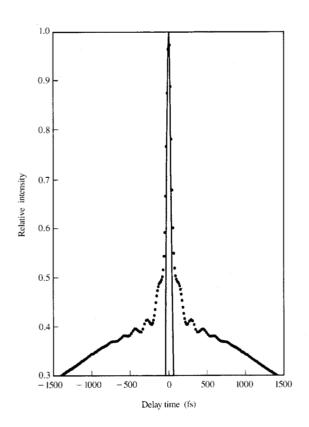


Figure 8 Transmission-correlation trace for Malachite Green.

simple model. If the dephasing time of the molecular vibrational wave packet is long compared to the pulse width, the transmission as a function of the delay of the probe pulse will be modulated by the oscillating coherent vibrational wave packet of the molecule. A detailed density matrix theory of this type of quantum beat effect is given in [2, 3].

In principle, the vibrational states in the ground electronic level can also lead to quantum beats through the resonant Raman process. In this case, the first optical pulse leaves the molecules in a coherent-superposition vibrational state in the ground electronic level. The subsequent oscillation of this coherent wave packet will modulate the probe pulse leading quantum beats. This effect is related to the impulsive stimulated Raman scattering (ISRS) [15]. Detailed discussions of the similarities and differences between these effects can be found in [16, 17].

Figure 8 shows the quantum beats observed in Malachite Green, which is the first observation of quantum beats in the femtosecond time domain. Similar beats have been seen in a number of other dye molecules. The amplitude, damping

Table 2 Summary of decay parameters for photoexcited organic dye molecules. The amplitudes are normalized so that y(t = 0) = 1.

$y(t) = \sum a_i \exp(-t/T_i) \cos(2\pi\nu_i t + \phi_i)$						
Molecule	a	T (fs)	ν (THz)	ϕ (degrees)		
Malachite Green	0.58 0.36 0.06	75 4800 205	6.60	11		
Ethyl Violet	0.60 0.33 0.07	120 1700 380	6.45	7		
Methyl Violet	0.55 0.23 0.19 0.03	39 2650 150 280	6.40	7		
Victoria Blue	0.57 0.31 0.11 0.01	30 10 000 105 190	6.14	13		
Methylene Blue	0.98 0.01 0.002	27 1470 380	7.7	2		
DODCI	0.47 0.32 0.09 0.07 0.03 0.02	185 1050 370 300 180 500	0.87 6.35 2.61 8.17 5.00	5 3 9 93 8		
Nile Blue	0.72 0.20 0.04 0.02 0.006 0.005 0.005 0.0007 0.0004 0.0003	43 400 180 490 560 405 4300 4700 3900 11 500	4.86 3.06 5.00 8.39 2.16 6.96 9.12 10.6	140 87 12 144 21 73 93 27		

constant, frequency, and phase of each component obtained using the linear-prediction procedure on the data for the molecules studied are shown in **Table 2**. In the cases of Malachite Green and Nile Blue, conventional Raman scattering experiments [18, 19] have confirmed that the observed beat frequencies correspond to particular vibrational frequencies of the molecules, consistent with the coherent wave-packet excitation model.

It is important to note that the decay of the quantum beats corresponds to the dephasing time of the wave packet and is independent of the optical dephasing time. In terms of the simple three-level model shown in **Figure 7(b)**, the optical dephasing time refers to the optical dipole moments corresponding to the transitions between levels 1 and 2 or 1 and 3. The dephasing time of the wave packet refers to the coherence between vibrational levels 2 and 3. Thus, quantum beats can be used to measure the dephasing time

between excited states in the presence of very rapid homogeneous or inhomogeneous optical dephasing. This is also true if the coherent wave packet is in the ground electronic level, as shown schematically in **Figure 7(c)**.

Conclusion

In conclusion, optical correlation spectroscopy coupled with the linear prediction procedure is capable of yielding quantitative results on the relaxation dynamics of nonequilibrium carriers in semiconductors and of photoexcited molecules. The basic technique and main results on GaAs and related compounds and structures and on a variety of dye molecules have been summarized and reviewed in this paper.

Acknowledgment

This work is supported by the National Science Foundation and the Joint Services Electronics Program.

References

- A. J. Taylor, D. J. Erskine, and C. L. Tang, J. Opt. Soc. Amer. B 2, 663 (1985).
- 2. M. Mitsunaga and C. L. Tang, *Phys. Rev. A* 35, 1720 (1987).
- I. A. Walmsley, M. Mitsunaga, and C. L. Tang, *Phys. Rev. A* 38, 4681 (1988).
- F. W. Wise, M. J. Rosker, G. L. Millhauser, and C. L. Tang, J. Quant. Electron. QE-23, 1116 (1987).
- E. P. Ippen and C. V. Shank, in *Ultrashort Light Pulses*, S. Shapiro, Ed., Springer-Verlag, New York, 1977.
- T. F. Heinz, S. L. Palfrey, and K. B. Eisenthal, Opt. Lett. 9, 359 (1984)
- H. Barkhuijsen, R. deBeer, W. M. Bovee, and D. van Ormondt, J. Mag. Res. 61, 465 (1985).
- M. J. Rosker, F. W. Wise, and C. L. Tang, Appl. Phys. Lett. 49, 1726 (1986).
- D. W. Bailey, C. J. Stanton, M. A. Artaki, K. Hess, C. L. Tang, and F. W. Wise, Solid State Electron. 31, 467 (1988).
- F. W. Wise, I. A. Walmsley, and C. L. Tang, Appl. Phys. Lett. 51, 605 (1987).
- C. J. Stanton, D. W. Bailey, K. Hess, and Y. C. Chang, *Phys. Rev. B* 37, 6575 (1988).
- D. J. Erskine, A. J. Taylor, and C. L. Tang, Appl. Phys. Lett. 45, 1209 (1984).
- M. J. Rosker, F. W. Wise, and C. L. Tang, *Phys. Rev. Lett.* 57, 321 (1986).
- F. W. Wise, M. J. Rosker, and C. L. Tang, J. Chem. Phys. 86, 2827 (1987).
- S. Ruman, A. G. Joly, and K. A. Nelson, *J. Chem. Phys.* 86, 6563 (1987); D. McMorrow, W. Lotshaw, and G. Kenney-Wallace, *J. Quant. Electron.* QE-24, 443 (1988).
- 16. A. Mokhtari and J. Chesnoy, Europhys. Lett. 5, 523 (1988).
- I. A. Walmsley, F. W. Wise, and C. L. Tang, Chem. Phys. Lett. 154, 315 (1989).
- K. A. Nelson and L. Williams, *Phys. Rev. Lett.* 58, 745(C) (1987).
- J. Ha, M. Marris, W. Risen, J. Tauc, C. Thomson, and Z. Vardeny, *Phys. Rev.* 57, 3302(C) (1986).

Received November 17, 1988; accepted for publication January 3, 1989

C. L. Tang Department of Electrical Engineering, Cornell University, Ithaca, New York 14853. Dr. Tang received his B.S. from the University of Washington, Seattle, in 1955; his M.S. from the California Institute of Technology, Pasadena, in 1956; and his Ph.D. from Harvard University, Cambridge, in 1960. He was a John Parker Traveling Fellow from Harvard University at the Technical University, Aachen, FRG, in 1959-1960. From 1960 to 1964 he was a Research Staff Member and later Principal Research Scientist with the Research Division of Raytheon Company. Dr. Tang joined the Cornell faculty as an Associate Professor in 1964 and has been Professor of Electrical Engineering since 1968 and a Chair Professor since January 1985. He is also a member of the Cornell Materials Science Center. During his sabbatical leave in 1970-1971, he was an NSF Senior Postdoctoral Fellow at Harvard and a consultant at the Naval Research Laboratory. In 1979-1980, he was a Visiting Professor at the University of Washington and a Scientific Consultant-at-Large at the Laboratoire d'Optique Quantique du C.N.R.S. in Paris. He was a Visiting McKay Professor at the University of California at Berkeley in 1985. Dr. Tang edited the volume on Quantum Electronics in the Methods of Experimental Physics series and was co-editor of the volumes on Nonlinear Optics in the Treatise on Quantum Electronics, both published by Academic Press. He has been an Associate Editor of the IEEE Journal of Quantum Electronics and is an Associate Editor of Optics Letters. Dr. Tang is a member of Phi Beta Kappa and Tau Beta Pi, and a Fellow of the American Optical Society, the American Physical Society, and the Institute of Electrical and Electronics Engineers. He was elected a member of the National Academy of Engineering in 1986.

Frank W. Wise Department of Applied Physics, 212 Clark Hall, Cornell University, Ithaca, New York 14853. Dr. Wise received a B.S. degree from Princeton University in 1980, an M.S.E.E. degree from the University of California, Berkeley, in 1982, and a Ph.D. in applied physics from Cornell University in 1988. During 1982 and 1983 he worked in advanced VLSI development at Bell Laboratories, Murray Hill, New Jersey. After completing his doctoral studies, Dr. Wise joined the faculty in Applied Physics at Cornell.

Mark J. Rosker Department of Physics, California Institute of Technology, Pasadena, California 91125. Dr. Rosker received the B.S. degree in physics from the California Institute of Technology in 1981, and the M.S. and Ph.D. degrees in applied and engineering physics from Cornell University in 1983 and 1987, respectively. His doctoral research was divided between the areas of nonlinear optics, including the development of a urea optical parametric oscillator, and ultrafast phenomena, in which the femtosecond energy relaxations of both semiconductors and organic molecules were studied. Since 1986, Dr. Rosker has been a Postdoctoral Research Fellow at the California Institute of Technology, where he is engaged in research aimed at observing the dynamics of unimolecular chemical reactions in real time.

I. A. Walmsley The Institute of Optics, University of Rochester, Rochester, New York 14627. Dr. Walmsley received the B.Sc (1st Class) in physics from Imperial College, University of London, and a Ph.D. in optics from The Institute of Optics, University of Rochester. His dissertation concerned macroscopic manifestations of quantum noise in stimulated light scattering. As a Postdoctoral Research Associate in the group of Professor C. L. Tang at Cornell University, he collaborated in studies of the short-time relaxation of photoexcited electrons in semiconductors and molecules. Dr. Walmsley was recently appointed an Assistant Professor in The Institute of Optics, where he is studying coherent optical interactions on extremely short timescales.